

Induced-fit Movements in Adenylate Kinases

Georg E. Schulz, Christoph W. Müller and Kay Diederichs

*Institut für Organische Chemie und Biochemie der Universität
Albertstrasse 21, D-7800 Freiburg i.Br., F.R.G.*

(Received 12 December 1989; accepted 28 February 1990)

The high-resolution crystal structures of three homologous adenylate kinases with zero, one and both (= 2-substrate mimicking inhibitor) bound substrates have been compared. The comparisons are meaningful, because all structures occur in two or three different crystal contact environments indicating that they represent intrinsically stable conformations in solution. Molecular superimpositions revealed that two domains comprising 30 and 38 residues undergo large movements on substrate binding, which can be approximated by rigid-body rotations over 39° and 92°, respectively. Moreover, these movements can be subdivided into two steps: first, a change on binding substrate AMP, which involves only the 30 residue domain (C α shifts up to 8.2 Å), and second, a change on additional binding of substrate ATP, which again involves the 30 residue domain (C α shifts up to 7.6 Å) but also the 38 residue domain (C α shifts up to 32.3 Å). Taken together, these observations yield a three-picture "moving film" of the induced-fit.

Kinases have to shield their catalytic centers against omnipresent water to avoid becoming ATPases (Jencks, 1975). For this purpose, kinases undergo an induced-fit (Koshland, 1958) as for instance observed for hexokinase (McDonald *et al.*, 1979; Bennett & Steitz, 1980). Here, we report on adenylate kinases (EC 2.7.4.3, $M_r = 21,000$ to 25,000) catalyzing the reaction $ATP + AMP \rightleftharpoons 2 ADP$ (Schulz *et al.*, 1986). We compare three high-resolution crystal structures with zero, one and both (= 2-substrate mimicking inhibitor) bound substrates and conclude that the immense differences are correlated with substrate binding.

The three crystal structures are listed in Table 1. Our conclusions are based on the following assumptions: (1) all adenylate kinases work in the same manner so that we can compare homologous enzymes; (2) the inhibitor Ap_5A^\dagger (i.e. ATP and AMP connected by an additional phosphate) mimicks the simultaneous binding of both substrates; (3) the observed crystal structures correspond to stable conformations of the enzyme and the enzyme-ligand complexes in solution.

Assumption (1) seems to be justified, since no

essential deviation has been detected in any of the steady-state kinetic analyses of adenylate kinase up to now. The enzymes AK1, AK3 and AKeco are clearly homologous, with 24% (AK1/AK3), 31% (AK1/AKeco) and 36% (AK3/AKeco) identical amino acid residues (Schulz *et al.*, 1986).

Assumption (2) seems justified because the binding mode of Ap_5A in AKeco (Müller & Schulz, 1988) is virtually identical with the mode observed with the yeast species (Egner *et al.*, 1987). Moreover, adenosine-B of Ap_5A (see Fig. 1(d)) corresponds to AMP as bound to AK3. That adenosine-A of Ap_5A corresponds to ATP, can be concluded from the structure of the GTP(GDP)-binding protein Haras-p21 (deVos *et al.*, 1988; Pai *et al.*, 1989). This G-protein shows close similarity with the adenylate kinases in the major part of the chain fold and especially in the glycine-rich loop. On the basis of the chain-fold similarity, bound GTP(GDP) in Haras-p21 superimposes with adenosine-A in AKeco.

There are strong indications that assumption (3) is correct. For AK1 we know two quite different crystal packings for the porcine and the carp enzyme (homology 74%) that have virtually the same structure with the deep cleft shown in Figure 1(a) (Reuner *et al.*, 1988). For AK3 and AKeco we observe two crystallographically independent molecules in the respective crystals (Table 1), and these have almost exactly the same structure (Table 2), although they form different packing contacts. Moreover, the conformation of Ap_5A -liganded AKeco is essentially identical with the corresponding structure of the yeast enzyme

\dagger Abbreviations used; Ap_5A , P^1, P^5 -bis(adenosyl-5'-)pentaphosphate; AK1, cytosolic adenylate kinase from vertebrates (here porcine muscle); AK3, adenylate kinase from the mitochondrial matrix (here bovine heart); AKeco, adenylate kinase from *Escherichia coli*; r.m.s., root mean square; INSERT, inserted domain in adenylate kinases; AMPbd, AMP-binding domain of adenylate kinases.

Table 1
Compared adenylate kinase structures

Enzyme	Enzyme species	Ligand	Number of residues	Precipitant ^a	pH	Resolution (Å)	Molecules per asymmetric unit	Space group
AK1 ^b	Porcine muscle cytosol	—	194	3.0 M-AS	7.7	2.1	1	<i>P</i> 3 ₁ 2 ₁
AK3 ^c	Bovine mitochondrial matrix	AMP	225	26% PEG	6.5	1.85	2	<i>P</i> 2 ₁ 2 ₁ 2 ₁
AKeco ^d	<i>Escherichia coli</i>	Ap ₅ A	214	2.5 M-AS	6.7	1.85	2	<i>P</i> 2 ₁ 2 ₂ 1

^a AS, ammonium sulfate; PEG, polyethylene glycol, average $M_r = 8000$.

^b The structure is refined to an *R*-factor of 19.3% including solvent (Dreusicke *et al.*, 1988).

^c After 18 rounds of simulated annealing (program XPLOR; Brünger *et al.*, 1987) the structure is presently refined to an *R*-factor of 18.9% including solvent. Details will be published elsewhere. This adenylate kinase (EC 2.7.4.10) uses GTP more efficiently than ATP.

^d After 13 rounds of simulated annealing using XPLOR (Brünger *et al.*, 1987) this structure is currently refined to an *R*-factor of 21.2% including solvent. The previous structure of INSERT (Müller & Schulz, 1988) has been modified. Details will be published elsewhere.

(Egner *et al.*, 1987; Müller & Schulz, 1988). Taken together, we consider all three assumptions justified, rendering the comparison meaningful.

In order to quantify the conformational differences between AK1, AK3 and AKeco, we first aligned the C^α backbones on a display (model PS-330; Evans & Sutherland, U.S.A.) such that the respective central parallel β -pleated sheets together with four helices on both sides of the sheets were fitted best. At these visual superimpositions, we assigned all residues as insertions that had no counterparts in the other structures. In addition we disregarded residues 133 to 141 of AK1 because of gross geometric deviations. The remaining 170 residues constituted an equivalenced set (residues 9 to 84, 86 to 87, 89 to 107, 109 to 132, 142 to 175, 177 to 191 of AK1; residues 6 to 126, 163 to 211 of AK3; residues 1 to 76, 78 to 98, 100 to 123, 160 to 186, 192 to 198, 200 to 214 of AKeco). The result differs from a previous sequence-based alignment (Schulz *et al.*, 1986; Egner *et al.*, 1987).

On the basis of this set, we determined the superpositions with the minimum root mean square (r.m.s.) distance between equivalenced C^α atoms using the program OVERLAY (cut-off 1 Å, 1 Å = 0.1 nm), which restricts the whole set to all atoms closer than the given cut-off (Kabsch, 1978). There remained 62 and 60 residues for the superimpositions AK3/AK1 and AKeco/AK1, respectively. Most of them were in the central β -sheet and in the four α -helices on both sheet sides. These superimpositions showed large deviations around residues 63 and 136 of AK1 (see above), both of which involved substantial parts of the chains.

The deviating segments were tentatively assigned by locating the residues where the general chain courses diverged. In a second step we superimposed the molecules on the deviating segments and located again the residues where the general chain courses diverged. In this way, bias from the sheet-centered superimposition described above was avoided. Since all points of divergence agreed well, we could clearly assign the deviating segments. They were named "AMP-binding domain" (AMPbd, residues 38 to 67 of AK1, 35 to 64 of AK3, 30 to 59 of AKeco) and

"inserted domain" (INSERT, residues 125 to 162 of AK3, 122 to 159 of AKeco; equivalent in AK1 is segment 131 to 141 that is 26 residues shorter than the other segments, giving rise to the name of the domain, and to the classification of AK1 as small and AK3 as well as AKeco as large adenylate kinase variants).

For determining the structural differences, we removed AMPbd and INSERT from the whole set of 170 residues, obtaining 138 equivalenced residues. This reduced set was used to superimpose AK3 on AK1 and AKeco on AK1 (OVERLAY, cut-off 1.5 Å). At the resulting orientations we then superimposed (OVERLAY, cut-off 1.5 Å) the respective domains AMPbd and INSERT to establish their relative deviations. The results are given in Table 2. The comparisons between the two non-crystallographically related molecules showed only small differences for the open structures of AK3 and almost no difference for the compact structures of AKeco. Therefore, we stated only a selection of all possible comparisons in Table 2; the others yield very similar numbers.

The resulting differences are large. They can be interpreted as a two-step movement. In the first step, which can be correlated to the binding of AMP, domain AMPbd of AK1 (with no substrate) closes down to AK3 (with bound AMP), the largest C^α movement being 8.2 Å (Fig. 1(a) and (b)). In the second step, which can be correlated to the additional binding of ATP, domain AMPbd of AK3 (bound AMP) closes further down to AKeco (with bound Ap₅A mimicking both substrates), the largest C^α movement being 7.5 Å. Comparing the AMPbd domains before the first and after the second step yields a maximum distance of 12.5 Å, which approximates the sum of the other differences. The corresponding polar rotation angles (Rossmann & Blow, 1962) add up similarly (Table 2). Also in the second step, domain INSERT of AK3 (bound AMP) closes down to AKeco (bound Ap₅A) covering the active center region as shown in Figure 1(c) and (d)). This movement is exceptionally large, INSERT rotates by 92°, the maximum C^α shift is 32.3 Å. It should be noted that the observed huge

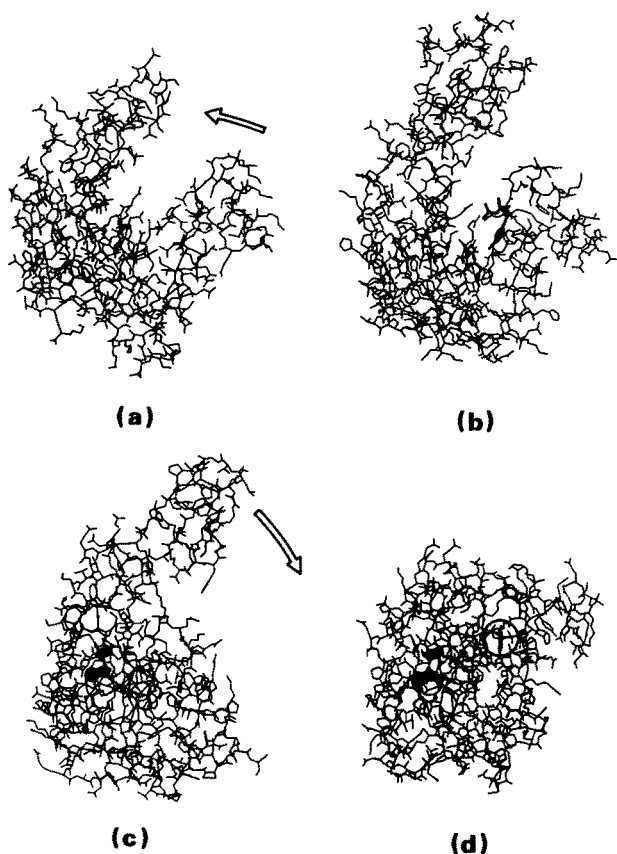


Figure 1. Domain movements correlated with substrate binding to adenylate kinases. The depicted models contain all non-hydrogen atoms. The movements are indicated by arrows. (a) Model of AK1 (Dreusické *et al.*, 1988) with no bound ligand showing a deep cleft poised to accept the substrates. (b) Model of AK3 with bound AMP viewed as superimposed on AK1 (see the text) but laterally separated. Given are residues 5 to 218; AMP, at the right-hand side of the cleft, is emphasized. The movement of domain AMPbd at the right-hand side is indicated in (a) and quantified in Table 2. (c) Model of AK3 with bound AMP after 90° rotation of (b) around a vertical axis. The model shows a broad cleft poised to bind ATP at its bottom. Domain INSERT stands out at the top. (d) Model of AKeco with bound Ap_5A viewed as superimposed on AK1 (see the text) and oriented as AK3 in (c). The 2-substrate mimicking inhibitor Ap_5A is emphasized. The purin and ribose rings of adenosine-B are filled in black, adenosine-A is marked by encircling. Domain INSERT has closed down over the substrates (here Ap_5A), the movement is indicated in (c) and quantified in Table 2.

movement of INSERT of the large adenylate kinase variants suggests that also the equivalent segment 131 to 141 of the small variant AK1 moves on binding both substrates.

Program OVERLAY represents domain movements as rigid-body rotations and translations. The deformations of the domains are merely described by the residual r.m.s. C^α distances, which are given in Table 2. For domain INSERT with 38 residues, the residual r.m.s. C^α distance is only 1.5 Å in spite of the large movement; accordingly the deformations are relatively small. The r.m.s. C^α distances for

AMPbd are 1.0 Å in the first step (AK1 to AK3), 1.6 Å in the second step (AK3 to AKeco) and 2.6 Å in a comparison of initial and final structure (AK1 to AKeco). Considering the smaller movements of AMPbd and the shorter segment (30 residues), these values indicate more substantial deviations from rigid-body movements.

All resulting rotations and translations are explicitly listed in Table 2. An interpretation according to Cox (1967) describes the rigid-body movement as a rotation around a particular polar axis coupled with a shift along this axis. The polar rotation angles are given in Table 2, they are defined as given by Rossmann & Blow (1962). All longitudinal shifts are small; for AMPbd they range between 0.3 Å and 0.5 Å, for INSERT the shift is 1.8 Å, indicating that the movements are essentially pure rotations. Furthermore, the polar axes transverse the proteins close to particular C^α atoms, which could therefore be considered as hinge positions. For INSERT these are at residues 123 and 161 of AK3 (distances 2 to 3 Å between C^α and axis). For AMPbd, we calculated three different rotations (Table 2), the polar axes of which deviated somewhat from each other, indicating that there is no well-defined hinge. The largest rotation (AK1 to AKeco) should have the most accurate polar axis. This axis traverses the molecule close to residues 34 and 65 of AKeco (distances between 1 and 2 Å).

In Figure 1(c) the protruding domain INSERT can be well recognized at the top, in Figure 1(d) it has closed down over the bound substrates giving rise to the rather globular molecule AKeco. This huge movement, which is here correlated with ATP-binding, may forecast the magnitude of the changes to be expected for myosin and F_1 -ATPase, which are homologous with the adenylate kinases at least in the ATP-binding glycine-rich loop (Dreusické & Schulz, 1986). They are appreciably larger than the conformational changes reported for hexokinase (Bennett & Steitz, 1980), alcohol dehydrogenase (Eklund *et al.*, 1981) and citrate synthase (Remington *et al.*, 1982; Bennett & Huber, 1984) as based on crystal structures and for arabinose-binding protein as derived from small angle X-ray scattering (Newcomer *et al.*, 1981).

Taking these results together, we observe in AK1, AK3 and AKeco three still pictures of the series of conformational changes from a substrate-free enzyme (here AK1) to its catalytically active form (here AKeco). It would be of interest to fill in more pictures, for instance by molecular dynamic calculations, in order to obtain a smoothly running "film" of this catalytic cycle. The reported data re-emphasize that there exists a broad spectrum of conformational changes during enzyme catalyses. Adenylate kinases with their immense mechanical movements for phosphoryl transfer appear to represent enzymes from steam-engine times to life evolution, in contrast to enzymes from silicon-chip times such as glutathione reductase, which transfer merely electrons and undergo only minimal movements during catalysis (Karplus & Schulz, 1989).

Table 2
Induced-fit movements of AMP-binding and inserted domains of adenylate kinases

	Domain	AK3-I ^a $\Delta C^{\alpha c}$ (Å)	κ^d (deg.)	r.m.s. $\Delta C^{\alpha d}$ (Å)	AKeco-I ^a $\Delta C^{\alpha c}$ (Å)	κ^d (deg.)	r.m.s. $\Delta C^{\alpha d}$ (Å)
AK1 ^b	AMPbd	8.2 ^e	24	1.0	12.5 ^f	39	2.6
AK3-II	AMPbd	2.6 ^g	8	0.3	7.5 ^h	18	1.6
	INSERT	2.8 ⁱ	9	0.2	32.3 ^j	92	1.5
AKeco-II	AMPbd	—	—	—	0.5 ^k	2	0.2
	INSERT	—	—	—	1.5 ^l	4	0.3

^a Roman numerals are used to identify the independent molecules in the asymmetric unit: the centers of mass of AK3-I and AKeco-I are (0.05, 0.55, 0.38) and (0.33, 0.57, 0.29) as given in fractional co-ordinates of the respective crystal.

^b For the comparison, the C^α backbone of AK3-I, -II and AKeco-I, -II have been superimposed on the C^α backbone of AK1 (Dreusicke *et al.*, 1988) applying the program OVERLAY (cut-off 1.5 Å) to the reduced set of 138 equivalenced C^α atoms (Kabsch, 1978; see the text). In a previous publication (Dreusicke & Schulz, 1988) the AK1 structure at pH 7.7 (Table 1) had been compared to the crystalline structure of the same AK1 at pH 5.8. The observed differences in AMPbd were much smaller than those discussed here.

^c Given are the largest C^α deviations in the respective domains, which correspond to the maximum C^α movements.

^d After the superimpositions onto AK1, the relative orientations of AMPbd and INSERT were determined by another run of OVERLAY (cut-off 1.5 Å) yielding the polar rotation angles κ (Rossmann & Blow, 1962) of the movements. The residual r.m.s. ΔC^{α} distance is also given. In order to allow the derivation of further parameters, the detailed rotation matrices and translations (ordered: $a_{11}, a_{12}, a_{13}, a_{21}, \dots; b_1, b_2, b_3$) are given under footnotes e to l below. Applying the transformations on domains AMPbd and INSERT of AK3-I and AKeco-I (head row) superimposes these onto the respective domains of AK1, AK3-II and AKeco-II (first column). The translations (b_1, b_2, b_3) are the vectors between the respective centers of gravity.

^e Transformation: 0.9151, 0.2719, 0.2977, -0.2949, 0.9549, 0.0342, -0.2749, -0.1191, 0.9541; 2.4, -2.0, -1.9.

^f Transformation: 0.7729, 0.2339, 0.5899, -0.2484, 0.9669, -0.0579, -0.5839, -0.1017, 0.8054; 5.6, -1.3, -4.7.

^g Transformation: 0.9910, -0.0074, 0.1337, 0.0093, 0.9999, -0.0133, -0.1336, 0.0144, 0.9909; 0.7, 0.0, -1.2.

^h Transformation: 0.9529, -0.0078, 0.3032, 0.0257, 0.9982, -0.0551, -0.3022, 0.0603, 0.9513; 2.7, 0.0, -3.9.

ⁱ Transformation: 0.9955, 0.0002, -0.0945, 0.0119, 0.9919, 0.1268, 0.0938, -0.1274, 0.9874; -1.0, 0.6, 0.5.

^j Transformation: 0.8683, 0.2760, -0.4122, 0.4002, 0.1012, 0.9108, 0.2931, -0.9558, -0.0226; 0.7, 6.7, 18.3.

^k Transformation: 0.9997, 0.0250, -0.0055, -0.0249, 0.9997, 0.0091, 0.0057, -0.0089, 0.9999; 0.0, -0.2, -0.1.

^l Transformation: 0.9975, 0.0508, 0.0483, -0.0505, 0.9987, -0.0070, -0.0486, 0.0046, 0.9988; -0.3, 0.1, 0.1.

References

- Bennett, W. S., Jr & Steitz, T. A. (1980). *J. Mol. Biol.* **140**, 211–230.
- Bennett, W. S., Jr & Huber, R. (1984). *CRC Crit. Rev. Biochem.* **15**, 291–384.
- Brünger, A. T., Kuriyan, J. & Karplus, M. (1987). *Science*, **235**, 458–460.
- Cox, J. M. (1967). *J. Mol. Biol.* **28**, 151–156.
- deVos, A. M., Tong, L., Milburn, M. V., Matia, P. M., Jancarik, J., Noguchi, S., Nishimura, S., Miura, K., Ohtsuka, E. & Kim, S.-H. (1988). *Science*, **239**, 888–893.
- Dreusicke, D. & Schulz, G. E. (1986). *FEBS Letters*, **208**, 301–304.
- Dreusicke, D. & Schulz, G. E. (1988). *J. Mol. Biol.* **203**, 1021–1028.
- Dreusicke, D., Karplus, P. A. & Schulz, G. E. (1988). *J. Mol. Biol.* **199**, 359–371.
- Egner, U., Tomasselli, A. G. & Schulz, G. E. (1987). *J. Mol. Biol.* **195**, 649–658.
- Eklund, H., Samama, J.-P., Wallen, L., Bränden, C.-I., Åkeson, A. & Jones, T. A. (1981). *J. Mol. Biol.* **146**, 561–587.
- Jencks, W. P. (1975). *Advan. Enzymol.* **43**, 219–410.
- Kabsch, W. (1978). *Acta Crystallogr. sect. A*, **34**, 827–828.
- Karplus, P. A. & Schulz, G. E. (1989). *J. Mol. Biol.* **210**, 163–180.
- Koshland, D. E., Jr (1958). *Proc. Nat. Acad. Sci., U.S.A.* **44**, 98–104.
- McDonald, R. C., Steitz, T. A. & Engelman, D. M. (1979). *Biochemistry*, **18**, 338–342.
- Müller, C. W. & Schulz, G. E. (1988). *J. Mol. Biol.* **202**, 909–912.
- Newcomer, M. E., Lewis, B. A. & Quioco, F. A. (1981). *J. Biol. Chem.* **256**, 13218–13222.
- Pai, E. F., Kabsch, W., Krengel, U., Holmes, K. C., John, J. & Wittinghofer, A. (1989). *Nature (London)*, **341**, 209–214.
- Remington, S., Wiegand, G. & Huber, R. (1982). *J. Mol. Biol.* **158**, 111–152.
- Reuner, C., Hable, M., Wilmanns, M., Kiefer, E., Schiltz, E. & Schulz, G. E. (1988). *Protein Seq. Data Anal.* **1**, 335–343.
- Rossmann, M. G. & Blow, D. M. (1962). *Acta Crystallogr.* **15**, 24–31.
- Schulz, G. E., Schiltz, E., Tomasselli, A. G., Frank, R., Brune, M., Wittinghofer, A. & Schirmer, R. H. (1986). *Eur. J. Biochem.* **161**, 127–132.

Edited by R. Huber